Anomalous dynamic scaling of Ising interfaces

Enrique Rodríguez-Fernández,[1, *] Silvia N. Santalla,[2, †] Mario Castro,[3, ‡] and Rodolfo Cuerno[4, §]

[1]*Departamento de Matemática Aplicada y Ciencias de la Computación and Grupo Interdisciplinar de Sistemas Complejos (GISC),
Universidad de Cantabria, Avenida de los Castros s/n, 39005 Santander, Spain*
[2]*Departamento de Física and GISC, Universidad Carlos III de Madrid, Avenida de la Universidad 30, 28911 Leganés, Spain*
[3]*Instituto de Investigación Tecnológica (IIT) and GISC,
Universidad Pontificia Comillas, 28015 Madrid, Spain*
[4]*Departamento de Matemáticas and GISC, Universidad Carlos III de Madrid, Avenida de la Universidad 30, 28911 Leganés, Spain*

Until very recently, the asymptotic occurrence of intrinsic anomalous scaling has been expected to require concomitant effects for kinetically rough interfaces, like quenched disorder or morphological instabilities. However, counterexamples have been recently reported for simpler situations dominated by time-dependent noise, as in the discrete growth system associated with an Ising model proposed by H. Dashti-Naserabadi *et al.* [Phys. Rev. E **100**, 060101(R) (2019)], who assessed the equilibrium behaviour of the model. Here, we revisit this system to characterise its time-dependent behaviour in two and three dimensions (one- and two-dimensional interfaces, respectively). While the 3D case seems dominated by a fast evolution beyond critical dynamics, in the 2D case, numerical simulations of an associated time-dependent Ginzburg-Landau equation retrieve the same static (roughness) exponents and the same intrinsic anomalous scaling ansatz as in the equilibrium case throughout the complete time evolution. However, the dynamic exponent is seen to cross over between two different values, none of which enables identification with previously known universality classes of kinetic roughening. Moreover, simulations for larger system sizes suggest a breakdown of scaling behaviour at the largest scales, suggesting that the previously reported scaling behaviour may be effective and restricted to relatively small systems.

I. INTRODUCTION

Many spatially-extended systems of a high current interest operate under non-equilibrium conditions, from active [1, 2] to quantum matter [3, 4]. In these and many other contexts, the conditions for and the properties of the emergence of the strong correlations associated with space-time criticality [5] become relevant. From this point of view, a particularly interesting class of systems is that for which critical behaviour appears spontaneously without the need for parameter tuning, thus showing so-called generic scale invariance (GSI) [6, 7].

Surface kinetic roughening [8, 9] is a celebrated physical instance of GSI. Indeed, in many different systems, from thin film production to bacterial colonies, the fluctuations of rough surfaces and interfaces are observed to evolve in the absence of typical scales in time and space. To date, some of the main universality classes of surface kinetic roughening, like that of the Kardar-Parisi-Zhang (KPZ) equation [10], are held as paradigms of nonequilibrium critical phenomena at large [11–14], being surprisingly relevant even in contexts far away from those that motivated their original formulation. An example is the recent experimental observation of KPZ scaling for quantum condensates [15] and spin chains [16], the equation being originally formulated for non-quantum systems [8–10].

In general, the study of surface kinetic roughening remains instrumental in generalizing the concepts and tools of equilibrium critical dynamics to systems which are far from equilibrium [11–14]. A crucial ingredient at this has been the dynamic scaling ansatz satisfied by the relevant physical quantities, such as the surface roughness and correlations. As seminally proposed by Family and Vicsek (FV) [17], it is a direct generalization of the dynamic scaling ansatz of equilibrium critical dynamics found in e.g. the classic models A and B [5, 18]. Indeed, the so-called FV ansatz is satisfied e.g. by the KPZ equation and by many other systems displaying kinetic roughening [8, 9]. However, generalizations of the FV ansatz, collectively termed anomalous scaling [9, 19–22], have been later shown to be required to account for more elaborate scaling behaviour found in models and in experiments, whereby e.g. different critical exponents characterise fluctuations at distances smaller than or comparable to the system size.

Up to quite recently, one of these generalised *ansatzs*, the so-called intrinsic anomalous scaling, was believed (following a conjecture [24] based on renormalization group arguments) to occur asymptotically for some rough interfaces only when subject to relatively peculiar conditions, like quenched disorder and/or morphological instabilities. Hence, the observation of intrinsically anomalous scaling in the equilibrium state of a growth system related with a critical Ising model [25] comes as a surprise, since no such peculiarities are apparent in the system formulation.

Notably, the values of the static scaling exponents and the scaling ansatz verified in Ref. [25] coincide with those found very recently for the tensionless KPZ equation (TKPZ), a particular case of the KPZ equation and thus a candidate continuum representative of the universality class exposed by the results in Ref. [25]. The TKPZ equation has attracted recent interest for 1D interfaces [26–29], not the least for its potential relevance for non-KPZ scaling behaviour experimentally found in some KPZ-related systems [15, 16]. Actually, the
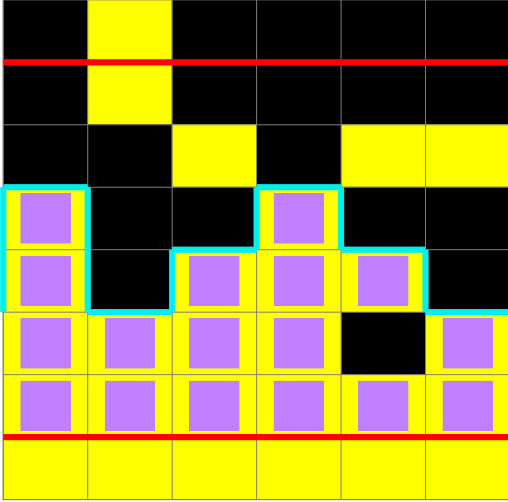
FIG. 1: Definition of the height profile $h(x)$ (cyan solid line) from a certain 6×6 Ising spin domain. See full definitions in Sec. III of the main text. Yellow and black cells correspond to $+1$ and -1 spin values, respectively. The spin rows below and above the bottom and top red lines illustrate the Dirichlet and Neumann boundary conditions, respectively. The (yellow) cells making up the cluster connected to the Dirichlet boundary via nearest neighbours are indicated by a purple square. The value of $h(x)$ corresponds to the height of the topmost one of such marked cells for each x.

1D TKPZ equation has been shown to define a universality class of its own [27, 28], different from that of the standard KPZ equation, which encompasses scaling behaviour earlier found for e.g. growth models related with isotropic percolation [30, 31]. The TKPZ equation seems to be the first continuum model displaying intrinsically anomalous scaling [27, 28] in absence of quenched noise or morphological instabilities.

In this work, we revisit the interface growth model proposed in Ref. [25]. As the authors of that reference were addressing equilibrium properties of their system, specifically its classical roughening transition, no time-dependent behaviour was reported and the kinetic roughening behaviour was extracted from the system-size dependence of correlation functions. Thus, our goal is to study the time-dependent behaviour of the system. Specifically, in our present work we study the full dynamics of the growth process defined in Ref. [25] at the critical temperature, $T = T_c$. We perform numerical simulations of the evolution of Ising spin domains in 2D and 3D, using both a Metropolis algorithm and an alternative coarse-grained approach based on the Ginzburg-Landau equation, using the boundary conditions proposed in Ref. [25] and described in Fig. 1.

This paper is organised as follows. In section II, we describe the observables we will measure to characterise the scaling of kinetic roughening processes. In section III, we describe the boundary conditions of the Ising model we will deal with, the definition of the interface, and the two different approaches that we have followed for the simulation of the time evolution of the system. Then, we describe the numerical results obtained both for 1D and 2D fronts (related to 2D and 3D Ising systems, respectively) via our Ginzburg-Landau approach in sections IV and V. The results obtained via a Metropolis Monte Carlo approach are presented in Appendix A. We discuss our results in section VI, followed by a summary and our conclusions in section VII. Appendices B and C contain further details on parameter choices and additional numerical results, respectively.

II. OBSERVABLES

The observables which are going to be used in the characterization of the front dynamics are *(i)* the global roughness,

$$W(t) = \left\langle \sqrt{\frac{1}{L^d} \int_{[0,L]^d} [h(\vec{x},t) - \bar{h}(t)]^2 d\vec{x}} \right\rangle, \qquad (1)$$

where bar denotes spatial average, L is the lateral system size, and brackets denote the average over different realisations of the noise, *(ii)* the structure factor,

$$S(\vec{k},t) = \langle |\hat{h}(\vec{k},t)|^2 \rangle, \qquad (2)$$

where $\hat{h}(\vec{k},t)$ is the Fourier transform of $h(\vec{x},t)$ and $\vec{k}$ is d-dimensional wave vector, and *(iii)* the height-difference correlation function,

$$G_2(\vec{r},t) = \sqrt{\langle \overline{[h(\vec{x}+\vec{r},t) - h(\vec{x},t)]^2} \rangle}. \qquad (3)$$

In a kinetic roughening process [8], the global roughness scales with time as $W \sim t^\beta$ — with β being the so-called *growth* exponent — up to a saturation value $W_{sat} \sim L^\alpha$ which is reached at steady state. Here, α is the so-called *roughness* exponent, which is related to the fractal dimension of the front [8, 32]. The time t_{sat} required for the system to reach the steady state increases as $t_{sat} \sim L^z$. Here, $z = \alpha/\beta$ is the so-called *dynamic* exponent, which characterises the time dependence of the lateral correlation length ξ along the front as $\xi \sim t^{1/z}$ [8]. Frequently, time crossover behavior may occur whereby the system shows the scaling behavior of some universality class at short times while displaying a different one at longer times. An example is the KPZ equation itself, which displays linear, Edwards-Wilkinson (EW) properties early on in its dynamics, replaced by full-fledged nonlinear KPZ scaling at longer times [8]. Note that, in cases like this, the long-time scaling behavior may be impossible to see in small systems where saturation to steady state occurs before the asymptotic scaling has developed.

It is possible to define a scaling function f_W that summarizes the scaling laws of the roughness into the single expression [8, 17]

$$W(L,t) \sim L^\alpha f_W \left(\frac{t}{L^z} \right), \qquad (4)$$

provided,

$$f_W(u) \sim \begin{cases} u^\beta & \text{if } u \ll 1, \\ \text{constant} & \text{if } u \gg 1. \end{cases} \quad (5)$$

The local roughness measured over windows of size $l < L$ also scales with the window size l, with a local exponent α_{loc}. Equivalently, the height-difference correlation function, Eq. (3), scales as $G_2 \sim r^{\alpha_{loc}}$, where $r = |\vec{r}|$. In general, $\alpha_{loc} = \alpha$ (e.g. in the standard KPZ equation [8, 9]). However, there are some kinetic roughening systems in which the local and the global scalings of the roughness with the window size are different, i.e. $\alpha_{loc} \neq \alpha$. Such behaviour is called *anomalous scaling* or *anomalous kinetic roughening* [19–22]. The structure factor scales in this case as [22]

$$S(\vec{k}, t) \sim k^{-(2\alpha+d)} f_S(k^z t), \quad (6)$$

where f_S behaves as

$$f_S(u) \sim \begin{cases} u^{2\alpha+d} & \text{if } u \ll 1, \\ u^{2(\alpha-\alpha_s)} & \text{if } u \gg 1. \end{cases} \quad (7)$$

Here, α_s is an exponent conveniently measured in Fourier space which is equal to α_{loc} when $\alpha_{loc} < 1$ [22]. For $\alpha = \alpha_{loc}$, the behaviour described by Eqs. (6) and (7) corresponds to the standard Family-Vicsek scaling ansatz [8, 17]. As noted above, while intrinsic anomalous scaling had been conjectured, via perturbative arguments, not to be in the asymptotic regime of continuum models which feature local interactions and time-dependent noise [24], it has been recently found for some such systems [28].

Additionally, we will also check multiscaling behaviour, where higher moments of the height-difference correlation function, namely,

$$G_q(\vec{r}, t) = \langle |h(\vec{x} + \vec{r}, t) - h(\vec{x}, t)|^q \rangle^{1/q}, \quad (8)$$

do not scale with the same roughness exponent for different values of q, i.e. for which $G_q(r) \sim r^{\alpha_q}$ with a q-dependent α_q. In those cases, the morphologies are considered multi-affine [8]. This behaviour appears e.g. in surface growth models related to isotropic percolation [30, 31].

Finally, recent developments on kinetic roughening, mostly related to the KPZ equation (see e.g. Refs. [11–14] and other therein), demonstrate the nontrivial role of the statistics of the height fluctuations to unambiguously identify the universality class, beyond scaling exponent values. Here, we will assess the field statistics by computing the probability distribution function (PDF) of the height fluctuations, as well as the time-dependent skewness,

$$\mathcal{S}(t) = \frac{1}{W^3(t)} \left\langle \frac{1}{L^d} \int_{[0,L]^d} [h(\vec{x}, t) - \bar{h}(t)]^3 d\vec{x} \right\rangle, \quad (9)$$

and the time-dependent kurtosis,

$$\mathcal{K}(t) = \frac{1}{W^4(t)} \left\langle \frac{1}{L^d} \int_{[0,L]^d} [h(\vec{x}, t) - \bar{h}(t)]^4 d\vec{x} \right\rangle, \quad (10)$$

where W is the roughness of the $h(\vec{x}, t)$ field.

III. SYSTEM DESCRIPTION

The physical system that we study in this work is in principle the same as that proposed in Ref. [25]. We define a 1D (resp. 2D) interface or front $h(x)$ (resp. $h(x, y)$) from a 2D (3D) spin domain $\{s_{\vec{r}}\}$, where $s_{\vec{r}} = \pm 1$ are Ising spins and $\vec{r}$ takes values on a 2D (3D) square lattice of lateral size L. Dirichlet (fixed) and Neumann (free) boundary conditions are fixed on each boundary in the last coordinate of $\vec{r}$ (the "vertical" or "growth" one, z); specifically, $s_{\vec{r}} = +1$ (resp. $s_{\vec{r}'} = s_{\vec{r}}$) if $z = 0$ (resp. if $z' = L + 1$ and $z = L$). Periodic boundary conditions are considered in the other (transverse or substrate) dimensions. We will refer to these boundary conditions as *magnet*. Then, a set of values $\mathcal{C}_{\vec{r}}$ is defined, such that $\mathcal{C}_{\vec{r}} = 1$ if spin $s_{\vec{r}}$ is aligned with the $+1$ spins fixed at the Dirichlet bottom boundary, which are connected to each other via nearest-neighbour paths, and $\mathcal{C}_{\vec{r}} = 0$ otherwise. For a 2D spin system, the height of the interface at a fixed substrate coordinate x is finally defined as

$$h(x) = \max\{z \mid \mathcal{C}_{\vec{r}} = 1\}, \quad (11)$$

where $\vec{r} = (x, z)$. An illustrative 2D spin domain with $L = 6$ under these boundary conditions and its corresponding $h(x)$ interface profile is depicted in Fig. 1. An analogous procedure defines the height of the interface at a fixed substrate coordinate (x, y) for a 3D spin system, where $\vec{r} = (x, y, z)$.

A. Metropolis approach

The most straightforward method for studying the dynamical evolution of the spin configurations of a ferromagnetic system consists of the use of Monte Carlo simulations [33]. A Metropolis algorithm can be used to simulate the full evolution of the spin field. At the same time, the equilibrium state of the model described in the previous paragraph was studied in Ref. [25] using Wolff's algorithm. For each Monte Carlo step, one random spin in a position $\vec{r}$ is chosen and flipped with probability $P_{\vec{r}}$, such that

$$P_{\vec{r}} = \begin{cases} e^{-\Delta E_{\vec{r}}/k_B T} & \text{if } \Delta E_{\vec{r}} > 0, \\ 1/2 & \text{if } \Delta E_{\vec{r}} = 0, \\ 1 & \text{if } \Delta E_{\vec{r}} < 0, \end{cases} \quad (12)$$

where

$$H[\{s_{\vec{r}}\}] = -J \sum_{\vec{r}} s_{\vec{r}} \left(\sum_{\vec{r}' \in \mathcal{N}(\vec{r})} s_{\vec{r}'} \right) \quad (13)$$

is the Ising Hamiltonian, $\mathcal{N}(\vec{r})$ is the set of all the nearest-neighbours for the position $\vec{r}$ on the 2D or 3D square lattice, $J > 0$ is a ferromagnetic coupling, and k_B is Boltzmann's constant. Hence, $\Delta E_{\vec{r}} = 2J s_{\vec{r}} \left(\sum_{\vec{r}' \in \mathcal{N}(\vec{r})} s_{\vec{r}'} \right)$ is the energy change due to the spin flip at position $\vec{r}$. The time scale is set to $t = N/L^d$, where N is the number of Monte Carlo steps.
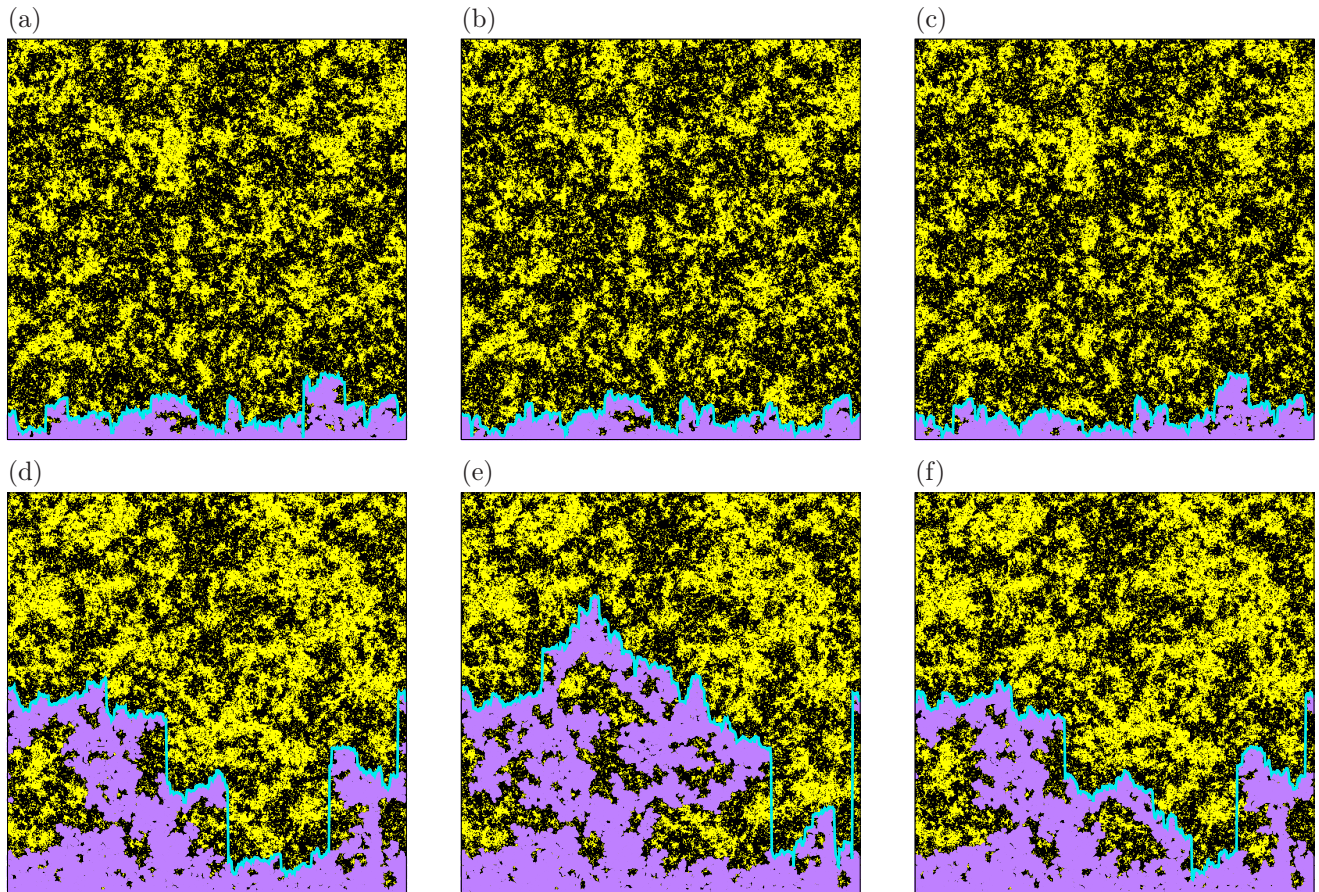
FIG. 2: Snapshots of the 2D spin domain obtained from a numerical integration of Eq. (14) for $L = 512$ and times $t = 403.1$, 403.2, and 403.3 for the top panels increasing from (a) to (c), and $t = 1099.3$, 1099.4, and 1099.5 for the bottom panels increasing from (d) to (f). The same colour coding of Fig. 1 is used here, with the only difference being that cells making up the cluster connected are now coloured fully in purple. Again, for each time the front $h(x, t)$ is shown as a cyan solid line. This front performs relatively large vertical jumps at all times. Moreover, its overall shape can change quite abruptly in relatively short intervals as illustrated e.g. by the (d)→(e)→(f) sequence.

This method yields a behaviour in which boundary effects strongly affect the evolution of the front h, so that its scaling can not be unambiguously assessed for the system sizes we have been able to simulate. The details of these results are described in Appendix A. In view of this fact, we alternatively employ a coarse-grained approach that allows us to access the effective behaviour of larger systems via the time-dependent Ginzburg-Landau equation.

B. Ginzburg-Landau approach

The (stochastic) Ginzburg-Landau (GL) equation [34]

$$\partial_t m = \frac{1}{2}\left(\nabla^2 m + m - m^3\right) + \tilde{D}\eta, \qquad (14)$$

where $m(\vec{x}, t)$ denotes the local magnetization field and η is an uncorrelated white noise term, is an effective coarse-grained model, well-known to describe the evolution of the scalar magnetization of an Ising ferromagnet around thermal equilibrium [34, 35]. We use this model in order to simulate the full dynamic evolution of our Ising system. We also define here a coarse-grained spin lattice $\{s_{\vec{x}}\}$ by discretizing $s_{\vec{x}} = +1$ if $m(\vec{x}) > 0$ and $s_{\vec{x}} = -1$ otherwise, from which we will define the field h as in the original spin system, recall Eq. (11). The same boundary conditions as those proposed in Ref. [25] are considered, see Fig. 1.

Our purpose is to assess the behaviour of this coarse-grained spin system at the noise amplitude value $\tilde{D} = \tilde{D}_c$ corresponding to the Ising critical temperature T_c. For such a value of the noise, the relative fluctuation of the local magnetization field,

$$M = \frac{\langle m^2(\vec{x})\rangle - \langle m(\vec{x})\rangle^2}{L^d \tilde{D}}, \qquad (15)$$

exhibits a divergence at steady state as $M \sim L^{\gamma/\nu}$. Here, $\gamma = 7/4$ and $\nu = 1$ are the exact Ising critical exponents in two dimensions [34] and $\gamma \simeq 1.23$ and $\nu \simeq 0.63$ are the approximate values in three dimensions [36].

Numerical simulations of Eq. (14) have been carried out in real space. A straightforward finite-difference scheme in

space and an Euler scheme in time have been employed [34], using $\Delta t = 0.1$ and $\Delta x = 1$. A homogeneous initial condition $m(\vec{x}) = -1$ is considered for all $\vec{x}$ except at the Dirichlet boundary, where $m = 1$ at all times.

IV. DYNAMICS AT $T = T_c$ FOR A ONE-DIMENSIONAL INTERFACE

A. $L \leq 2048$

The entire critical dynamics of the field $h(x,t)$ is evaluated at $\tilde{D} = \tilde{D}_c$. In Appendix B, $\tilde{D}_c \simeq 0.9$ is seen to correspond to the critical temperature $T = T_c$ of the 2D Ising model not only with periodic boundary conditions [34] but also with the magnet boundary conditions shown in Fig. 1.

Figure 2 shows snapshots of the 2D spin domain obtained in a sample realization of our numerical simulations of Eq. (14), which have been taken at increasing values of time from panel (a) through panel (f). The front $h(x,t)$ in each panel is shown as a cyan solid line. Such a line is seen to perform relatively many large vertical jumps. Its detailed shape can change quite dramatically in very short times when regions of the purple cluster connected to it by a few spins become "pruned" due to these spins flipping out of the cluster. This behaviour is even more dramatically seen in the movie available in the supplemental material (SM) at Ref. [37] and already anticipates large values for the scaling exponents, see e.g. Ref. [38] and other references therein.

1. Scaling exponents

Beyond surface morphologies, Fig. 3 shows the time evolution of both the surface roughness $W(t)$ and the structure factor $S(k,t)$, together with data collapses according to Eqs. (4) through (7). We find up to three different time regimes in the behavior of the roughness, which take place or not for a given value of L, depending on its size, recall the discussion right before Eq. (4) in Sec. II. In principle, small systems with $L < 2048$ saturate to an L-dependent steady state so that the saturated roughness value W_{sat} scales with L. Moreover, the smaller L is, the faster such a steady state is reached, as is standard in kinetic roughening conditions [8, 9]. However, for $L > 2048$ the steady state value W_{sat} ceases to scale with L, manifesting failure of kinetic roughening behavior.

More specifically, the three regimes found in Fig. 3(a) are: (1) for $0 < t < 10^2$ (values of time are approximate); (2) for $10^2 < t < 10^3$, and (3) for $t > 10^3$. Note that Ref. [25] employed system sizes $L \leq 2048$, which are explicitly addressed in the present paragraph for comparison. The behaviour we obtain for larger values of L up to $L = 8192$ is discussed in Sec. IV B below. For the smallest system size considered in Fig. 3 (namely, $L = 128$), the time increase of $W(t)$ is well characterised by a growth exponent value $\beta_1 \simeq 2/3$. Recalling that random deposition features $\beta_{RD} = 1/2$ [8], β_1 indicates very large interface fluctuations in time, as anticipated above. Furthermore, results for larger L values indicate

that this is a short-time behaviour followed by an even higher growth exponent $\beta_2 \simeq 3/2$ for sufficiently large system sizes. The transition from scaling regime 1 to scaling regime 2 in the time evolution of $W(t)$ takes place provided L is sufficiently large (say, $L \gtrsim 512$), being L-independent in such cases; compare the various $W(t)$ curves obtained for different L values in Fig. 3. This is analogous to, e.g., the well-known EW-to-KPZ time crossover displayed by the KPZ equation [8].

For intermediate L and times, one might measure an intermediate value of β close to that of the TKPZ equation ($\beta_{TKPZ} = 1$ [28]), but that is an apparent behaviour, as borne out from the data collapses of the structure factor. Indeed, for $L = 2048$ Fig. 3(c) shows that early time $S(k,t)$ data collapse well using $\alpha \simeq 1$ and $z_1 \simeq 3/2$ (hence, $\beta_1 = \alpha/z_1 = 2/3$), while Fig. 3(d) shows that long time data collapse well using $\alpha \simeq 1$ and $z_2 \simeq 2/3$ (hence, $\beta_2 = \alpha/z_2 = 3/2$). The $\alpha \simeq 1$ value is suggested by the system-size behaviour of the roughness at steady state [see the inset of Fig. 3(a) for $L \leq 2048$], while the spectral exponent value $\alpha_s \simeq 1/2$ describes the k-dependent behaviour of the structure factor, see Fig. 3(b). Indeed, recall that, in the presence of intrinsic anomalous scaling, Eqs. (6) and (7) imply that the structure factor scales as $S(k) \sim 1/k^{2\alpha_s + 1}$ for $k \gg 1/t^{1/z}$ [22]. Also, inspection of Fig. 2, suggests that the anomalous scaling may be due to the ocurrence of large *overhangs* that create large jumps in the interface. Such a behavior has also been shown to induce the (transient) appearance of intrinsic anomalous scaling in, e.g., a variant of the diffusion-limited aggregation model [23].

The intrinsically anomalous scaling ansatz which is verified and the roughness exponent values, $\alpha = 1$ and $\alpha_s = 1/2$, all coincide with those of the 1D TKPZ universality class [28], as also obtained in the simulations of Ref. [25]. Note, in the latter reference this scaling behaviour was obtained in equilibrium (at saturation, in our time-dependent approach), while we are presently assessing it along the time evolution of the system. However, in contrast with these TKPZ values for the roughness exponents, Fig. 3 rules out a ballistic value for the dynamic exponent z as in the TKPZ class, $z_{TKPZ} = 1$ [28]. For the sake of reference, the standard KPZ equation has a superdiffusive $z_{KPZ} = 3/2 < 2$ (as in our case for short times). Indeed, the value that we measure at long times, $z_2 = 2/3 < 1$, implies a spread of correlations that is even faster than ballistic, as occurs in the inviscid noisy Burgers equation [28]. It can also be found e.g. in suitable continuum models combining morphological instabilities with non-local interactions [39].

2. Statistics of front fluctuations

As noted above, beyond scaling exponent values the statistics of the height fluctuations is an additional trait of the system that identifies the kinetic roughening universality class. Hence, we next measure the fluctuations of the height field $h(x,t)$ at different times. Specifically, Fig. 4 shows our numerical results for the temporal evolution of the skewness, the kurtosis of the height fluctuations, and the full probability dis-
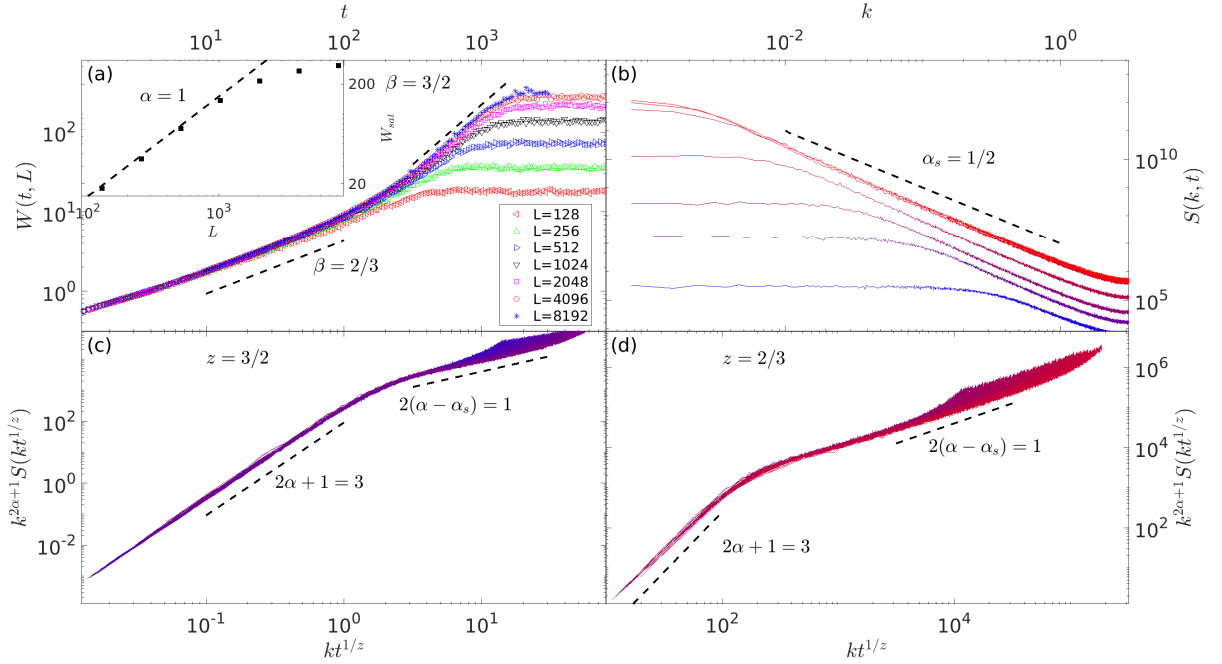
FIG. 3: Time evolution for (a) the roughness $W(t, L)$ and (b) the structure factor $S(k, t)$ of the field $h(x, t)$ defined from the simulations of Eq. (14) for a 2D domain. The inset in (a) shows the scaling of the saturation roughness W_{sat} with the system size L for the values of L given in the legend of the main panel. In (b) $L = 8192$ and time values increase bottom to top. These $S(k, t)$ data are collapsed in (c) [resp. (d)] for early [late] times during which $z = 3/2$ [$z = 2/3$] and $L = 2048$. Both collapses are for $\alpha = 1$ and $\alpha_s = 1/2$. In all panels, dashed lines correspond to the indicated values of the scaling exponents.

tribution function (PDF) of the steady-state fluctuations for our 1D fronts. Both $\mathcal{S}$ and $\mathcal{K}$ show very large values at short times which, after a nontrivial time evolution — frequently found in continuous nonlinear models —, eventually reach non-Gaussian (recall $\mathcal{S}_{\text{Gauss}} = 0$ and $\mathcal{K}_{\text{Gauss}} = 3$) values at steady state.

The full height PDF at saturation displayed in the inset of Fig. 4 is asymmetric indeed. We believe that the negative range of the fluctuations is over-represented due to a distortion introduced by the Dirichlet boundary condition at the bottom of the 2D domain. To illustrate the interplay of the morphology with the boundary conditions, we show in Fig. 9 the time evolution of the average mean height h, as well as the percentage of the individual realisations for which some parts of the $h(x, t)$ front reach the top boundary, thus influencing the fluctuations, for different values of the system size L. We observe how this percentage decreases with the system size, reaching a negligible value for $L = 2048$. Hence, the influence of the boundary in all measurements is expected to be very small for large system sizes.

3. Multiscaling

The morphologies in the nonlinear growth regime from the 2D GL model exhibit an abundance of prominent slopes to the naked eye, recall Fig. 3. In Fig. 6 we assess the PDF of

the slope field $u = \partial_x h$ for the GL interfaces. We observe in the figure that the tail of the PDF decays approximately as a power law $P(\chi_u) \sim \chi_u^{-2}$. In Ref. [30, 31], this type of slope statistics has been shown to imply multiscaling behaviour, as different q-moments of the height-difference distribution, Eq. (8), were then shown not to scale with the same roughness exponent α for different values of q. Specifically, in Refs. [30, 31], a surface growth model related to isotropic percolation (invasion percolation without trapping) was studied numerically, finding that the statistics were well described by the power law $P(\chi_u) \sim \chi_u^{-2}$. In that case, a scaling analysis based on isotropic percolation implies $\alpha_q = 1/q$ for arbitrary q. This seems to also be the case for $q > 1$ and not too large r in our present numerical simulations; see Fig. 7.

B. Larger values of L

As the reader may have noted when inspecting some of the figures presented in Sec. IV A 1, a still different behaviour (regime 3) is obtained for system sizes $L > 2048$. Starting with Fig. 3(a), the L-dependence of the saturation value of the roughness, W_{sat}, becomes weaker and becomes virtually nonexistent for our largest system size, $L = 8192$. A manifestation of this is the increasing deviation (for increasing L) of the effective $W_{sat} \sim L^\alpha$ law [see the inset of Fig. 3(a)], from the $\alpha \approx 1$ value obtained for $L \leq 2048$, towards an
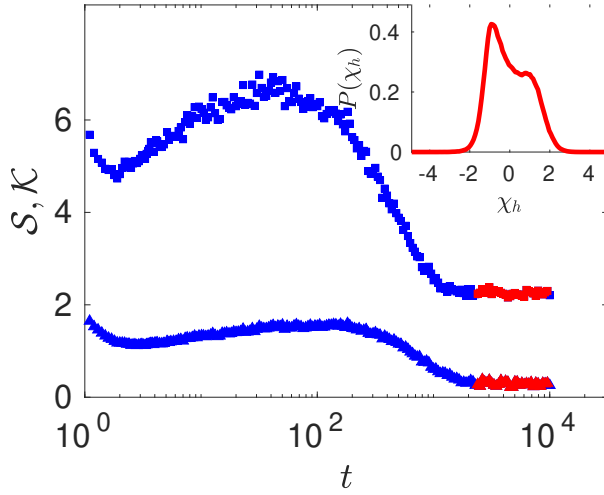
FIG. 4: Time evolution of the skewness (triangles) and kurtosis (squares) for the height fluctuations $\chi_h = (h - \bar{h})/\mathrm{std}(h)$ over 256 realisations from simulations of the GL model in 2D at critical noise $\tilde{D} = 0.9 \simeq \tilde{D}_c$ and $L = 2048$. The inset shows the full height PDF for times which correspond to the steady state, as implied by the behaviour of the skewness and kurtosis (red symbols).
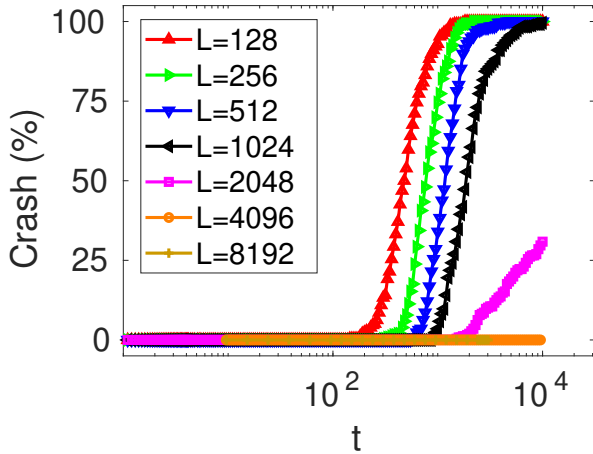

FIG. 6: Histogram of slope values [$\chi_u = (u - \bar{u})/\mathrm{std}(u)$, where $u = \partial_x h$] from morphologies of the 2D GL growth model for $L = 2048$ at steady state. The dashed black line corresponds to the indicated power-law behaviour with χ_u. Red dots correspond to the negative slopes.

FIG. 5: Percentage of single realisations in which the maximum height h has reached the system size L (which we denote by Crash) at any previous time for different values of L. For larger values ($L = 4196$ and $L = 8392$) it is equal to zero for all t.

FIG. 7: First, second, third, and fourth moments (bottom to top) of the height-difference correlation function $G_q(r)$ from numerical simulations of the 2D GL model in the nonlinear growth regime for $L = 2048$. Dashed straight lines correspond to the exact values of the slopes $\alpha_q = 1/q$, as predicted in Refs. [30, 31].

effectively null roughness exponent for the largest L, implying the breakdown of kinetic roughening (namely, the lack of scaling of W_{sat} with L) at large system size values. Indeed, the $W(t)$ data obtained for $L = 8192$ in the main panel of Fig. 3(a) largely fall on top of those obtained for $L = 4096$, essentially ruling out L-dependence of the roughness at such large system size values. This interpretation is reinforced by the $S(k,t)$ data displayed for $L = 8192$ in Fig. 3(b). Indeed, in the presence of kinetic roughening (and both, under a FV scaling ansatz and under an intrinsically anomalous
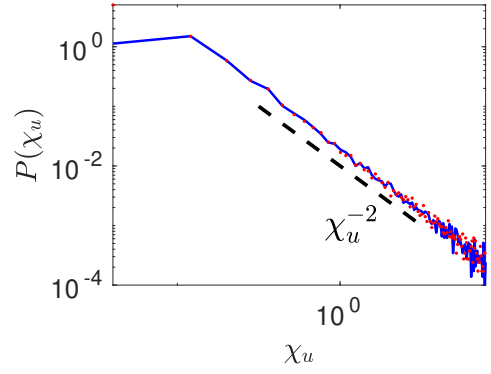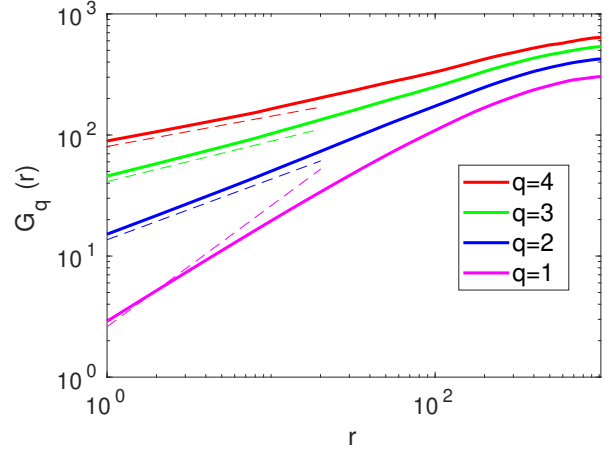
scaling ansatz), the value of $k_\times^* \sim 1/\xi(t)$ at which $S(k,t)$ changes from large-distance, uncorrelated, to short-distance, correlated behaviour moves towards $k = 0$ with increasing time. In contrast, the $S(k,t)$ curves in Fig. 3(b) become time-independent for the longest times and fall one on top of the other. In this case, the (inverse of the) corresponding value $k_\times^* \sim$ cnst. signals a time-independent characteristic lateral length scale instead of a time-dependent correlation length.
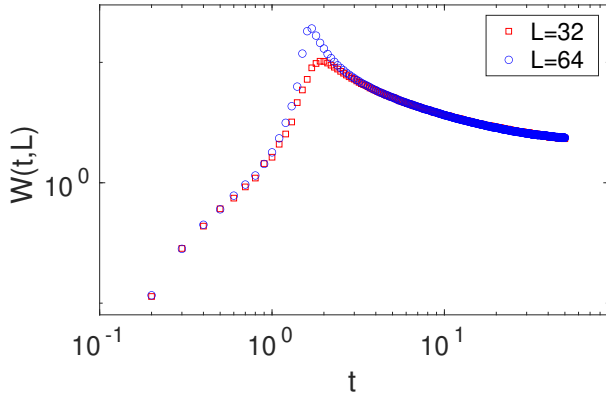
FIG. 8: Time evolution of the roughness W for the height profiles obtained from numerical simulations of the GL model in three-dimensional domains, using boundary conditions as described in Fig. 1, and for different values of the lateral system size L.
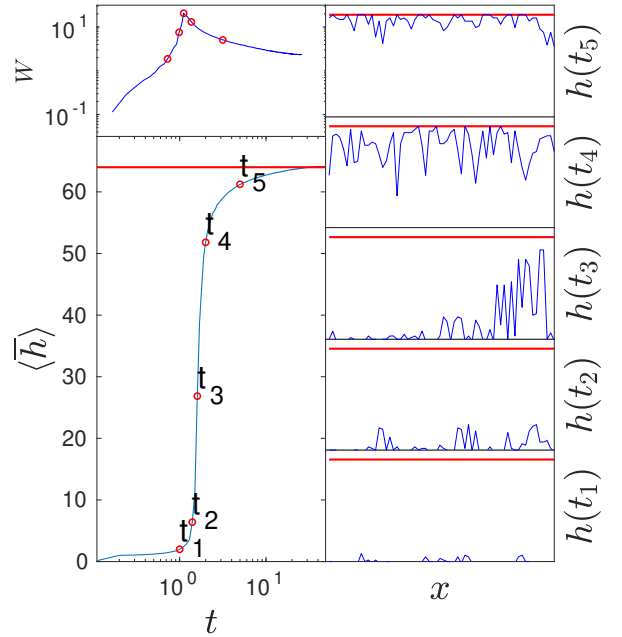

FIG. 9: Time evolution of the average mean height profile $\langle \bar{h} \rangle$ obtained over 10 realisations of the noise from numerical simulations of the 3D GL model (left bottom panel) compared to the maximum achievable height (domain lateral size, horizontal red solid line). Left top panel shows the corresponding evolution of the surface roughness $W(t)$. One realization of a longitudinal cut $h(x, 1, t)$ for each one of the highlighted times, t_1 to t_4 in the left panels, is shown in the right panels.

V.   DYNAMICS AT $T = T_c$ FOR A TWO-DIMENSIONAL INTERFACE

In this section, we study the dynamics of the spin configurations in three spatial dimensions, which lead to the time evolution of two-dimensional fronts or interfaces $h(x, y, t)$. The noise amplitude corresponding to the critical temperature in a 3D system is again assessed in analogy to our work for 2D spin domains. In this case, the critical $\tilde{D}$ takes the value $\tilde{D}_c \simeq 1.25$ [27].

Our main interest lies in the kinetic roughening properties of the corresponding $h(x, y, t)$ interfaces. The evolution of the front roughness $W(t)$ is depicted for different system sizes in Fig. 8. The growth of the roughness is suddenly interrupted and W starts to decay for $t \gtrsim 20$. This behaviour is induced by the upper boundary as we can appreciate in Fig. 9. Indeed, the mean height $\bar{h}$ suddenly approaches the upper boundary while the growth of the roughness is interrupted. The surface becomes pinned to this upper boundary for longer times, leading to a decrease in the roughness from that time on, much as it happens in our Metropolis approach for 1D and 2D fronts (see Appendix A). With our computational power, we have not been able to find L values which are free from this behaviour. Moreover, both under the GL approach and under the Monte Carlo approach assessed in Appendix A, the peak value for $W(t)$ reached in the 2D interfaces increases with the system size. Hence, we deem it unlikely that these crashes can be avoided for even larger L values than those considered here.

VI.   SUMMARY AND DISCUSSION

We have revisited the growth model formulated and studied in equilibrium in Ref. [25], to explore its time-dependent properties, aiming to assess asymptotic intrinsic anomalous scaling in a system with time-dependent noise. More specifically, in view of the reported anomalous scaling ansatz and

values of the roughness exponents [25], a natural hypothesis to be checked was if the dynamical exponent also agreed with that of the TKPZ equation, making the model a member of its universality class. In such a case, moreover, the discrete growth model might provide a means to explore that universality class in higher dimensions ($d > 1$) [40], where the continuum TKPZ equation is conspicuously prone to instabilities [27, 41, 42]. In our simulations, we have rephrased the model using a related stochastic, time-dependent Ginzburg-Landau equation.

For one-dimensional fronts, the model we are presently studying shows very strong fluctuations related to the definition of the spin cluster, which is linked with the spins located at the bottom boundary. Indeed, a few spin flips can suffice to attach/detach large spin subclusters, inducing strong variations in space and time for the front profile $h(x, t)$. Given the size of these fluctuations, a natural source of concern is whether our scaling results are determined by a prompt interaction with the upper boundary that confines the system. Still, Fig. 5 indicates that this is not the case for (sufficiently) large systems, including our largest values of L. For the smallest values of L, we demonstrate that the effect of the interaction with the upper boundary does not significantly perturb our results in Appendix C, were the full dynamics (data shown in Fig. 3) is reanalyzed by discounting all the realisations in which such an interaction occurs.

Continuing with 1D fronts, we have found that their scaling behaviour differs for $L \leq 2048$ (the range of L values studied in Ref. [25]) and for larger values of L. In the former case, during the full time evolution of the system, our model does reproduce the expected intrinsic anomalous scaling behaviour and the same numerical values of the roughness exponents ($\alpha = 1$ and $\alpha_s = 1/2$) of previous discrete (equilibrium) [25] and continuous [28] models. Actually, very similar kinetic roughening properties to these have been also measured [30, 31] in another discrete model of invasion percolation. Moreover, the surfaces in that model were seen to display similar $P(\chi_u) \sim \chi_u^{-2}$ slope statistics and multiscaling properties to those we are reporting in Figs. 6 and 7. However, this behaviour for the statistics of surface slopes, being absent in the continuum system studied in Ref. [28], is possibly related to the discrete nature of the surfaces and the single-valued approximation employed in the discrete models, as believed to be the case in other instances in the literature [43–47].

In spite of these similarities between the model we are studying and those in Refs. [28, 30, 31], the value of the dynamic exponent that we measure in our simulations crosses over in time between two different values, none of which coincide with the TKPZ value. In particular, the $z_2 = 2/3 < 1$ value measured at long times for $L \leq 2048$ indicates an extremely fast lateral spread of correlations (faster than ballistic) that preempts the eventual breakdown of scaling behavior seen for still longer times when $L > 2048$. Crossover behaviour of the present type, in which both the short and long time behaviours are intrinsically anomalous and only differ by the value of z, seems quite rare in the literature. Moreover, and as noted in Sec. I, the fact that the asymptotic behaviour remains intrinsically anomalous for a system with time-dependent noise contradicts theoretical expectations [24] based on (perturbative) renormalization group arguments for continuum models.

Related with the latter fact, our simulations of 1D fronts indeed show a different behaviour for $L > 2048$, which implies that the scaling found for smaller systems is not asymptotic. Indeed, as suggested by the behaviour of the roughness $W(t)$ and the surface structure factor $S(k,t)$, kinetic roughening seems to break down at sufficiently large distances and times. Very analogous behaviour has been recently reported for other kinetically rough systems [38]. Thus for instance, an off-lattice generalization of the ballistic deposition model [48], which has been shown to describe quite accurately [49] kinetically rough 1D fronts emerging in coffee-ring formation processes in colloidal systems [50–53], has been shown to display effective intrinsically anomalous scaling at small to intermediate scales; however, such a scaling behaviour breaks down at the largest time and length scales, being overridden by some sort of morphological instability inducing the formation of macroscopic shapes [38]. The intrinsic anomalous scaling becomes problematic in the $L \to \infty$ limit, as $S(k,L) \sim L^{2(\alpha - \alpha_s)}$; hence it is natural to expect it to be not an asymptotic behaviour but a transient in most real systems.

In the case of 2D fronts in our 3D Ising systems, we obtain a very fast increase of the surface roughness due to the fast evolution of the interface height, so that no non-trivial scaling behaviour develops. This is the case for both our Ginzburg-Landau and Metropolis approaches. Here, note that while Ref. [25] reports a 3D surface roughness that does scale (at equilibrium) with system size under analogous conditions, it does so as if the system was above the upper critical dimension, which is unexpected taking into account that 2D sections of that same system behave as the 1D interfaces of 2D Ising systems.

Considering the detailed dynamical behaviour that we obtain, the $\beta > 1/2$ exponent values observed for our 1D fronts at small to intermediate scales and the large-scale breakdown of kinetic roughening might be anticipating the singular behaviour that arises in higher dimensions. Recall that larger values of β are usually taken as indicative of morphological instabilities for systems with time-dependent noise, as $\beta = 1/2$ characterises the roughness increase for the random deposition process [8]. The TKPZ equation itself can be understood as being at onset of a morphological instability [28, 54], so that one might expect a suitable modification of it to account for the scaling behavior that we presently find. In view of the processes illustrated by Fig. 2, one possibility is that the local growth velocity may depend on the configuration of the system far away from the location where it is being computed, suggesting a potential role for nonlocal effects. In turn, these may induce morphological instabilities which may be described by an effective interface equation akin to that formulated for, e.g., in diffusion-limited growth, see Ref. [39] and other therein.

In our simulations, the description of the Ising system proposed in Ref. [25] seems feasible via the GL equation in the one-dimensional case. It has been extended to the study of the evolution of two-dimensional interfaces. However, the interaction of the interface with the free boundary of the system does not allow us to follow the long-time evolution in these 2D substrates. This is the case for the GL and the discrete approach to the dynamics based on our Metropolis algorithm. While we can avoid the crash between the interface and the upper boundary in the simulations of the 1D fronts by scaling up the effective system size through a coarse-grained approach, this seems impossible for the 2D fronts. Indeed, in the latter case, this phenomenon also occurs even under the coarse-grained GL approach, with the peak values for $W(t)$ increasing with the system size under both approaches.

VII. CONCLUSIONS

In conclusion, we have shown that the 1D interfaces defined over the Ising spin systems as in Ref. [25] do not feature asymptotic kinetic roughening for large systems sizes ($L > 2048$). For the previously explored range of L values ($L \leq 2048$), we do reproduce the intrinsically anomalous scaling ansatz and the values of the global and local roughness exponents obtained for the equilibrium discrete Ising model [25] and for some continuous systems [28]. In our present case, we have employed a Ginzburg-Landau approach to the dynamic behaviour of the Ising system which provides better results than those obtained from a simple Metropolis algo-

rithm. Still, the dynamic exponent crosses over in our simulations between short and long-time values, none of which agree with that of the TKPZ continuous model. The intrinsic anomalous scaling found for $L \leq 2048$ is perhaps related to non-localities in the interactions at play, e.g. the effect that single spin flips have in the dynamics of large regions of the front. In these cases the interface shows strong fluctuations with multiscaling and fat-tailed slope statistics — perhaps related to the discreteness of the spins and the single-valued approximation of the fronts—, all of which (except again for the value of z) agree with earlier discrete models of invasion percolation.

On the other hand, the 2D fronts obtained through our approach present a discrete version of "blow-up", which might be analogous to that reported for the continuous 2D tensionless KPZ equation [28, 41, 42]. In our 3D spin model, this "blow-up" is due to the interaction with the system boundaries and is reminiscent of analogous behaviour we have found for the 1D fronts of our smallest 2D systems. To extract more definitive conclusions on the behaviour of the 2D fronts (including the analysis of their symmetries [55], provided the universality class can be defined), improved simulations of our non-equilibrium system seem required which access substantially larger system sizes, perhaps via cluster algorithms akin to those employed at equilibrium. In this process, it would also be interesting to explore alternative boundary conditions to those that were originally implemented [25].
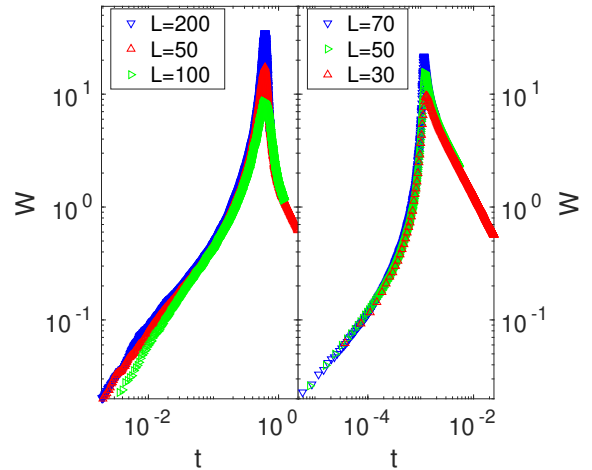
FIG. 10: Time evolution of the roughness W for the height profiles obtained in the Metropolis evolution of an Ising system in both, two and three-dimensional domains (left and right panels, respectively) with boundary conditions as described in Fig. 1 and for different values of the lateral system size L.

Appendix A: Simulation results using the Metropolis algorithm

The evolution of the interface field h defined as described in Section III, i.e. using Eqs. (11) and (12) for both, 2D and 3D spin lattices, has been measured at $T = T_c$, where $T_c = 2/\ln\left(1 + \sqrt{2}\right) \simeq 0.44$ is the exact value for the 2D square lattice and $T_c \simeq 0.22$ for the 3D cubic lattice [25].

We find very fast growth of the roughness W with time, as shown in Fig. 10 for different lateral system sizes L for both 2D and 3D spin domains, hence 1D and 2D fronts. Such a fast growth process is interrupted when the mean height approaches the boundary of the system, leading to an abrupt decrease in the roughness from that time on. This behaviour is very similar to that found in our Ginzburg-Landau approach for 3D domains, see Sec. V. As the GL equation provides a coarse-grained description involving continuum, instead of discrete, values of the local degrees of freedom, it might be describing effectively larger system sizes with a comparable computational cost.

Appendix B: Identification of the critical temperature

We assess the behaviour of the Ginzburg-Landau equation, Eq. (14), at different values of the noise strength D in order to determine the noise amplitude corresponding to the critical temperature T_c. In Fig. 11 we show how the relative fluctuation of the magnetization field — see Eq. (15) — at steady state $t \gg 1$ exhibits a divergence as $M \sim L^{\gamma/\nu}$ for the critical value $D = D_c \simeq 0.9$ corresponding to the critical temperature $T = T_c$. Here, $\gamma = 7/4$ and $\nu = 1$ are the Ising critical exponents in two dimensions [34]. This divergence is more clear if we consider a spin system in which all the boundary

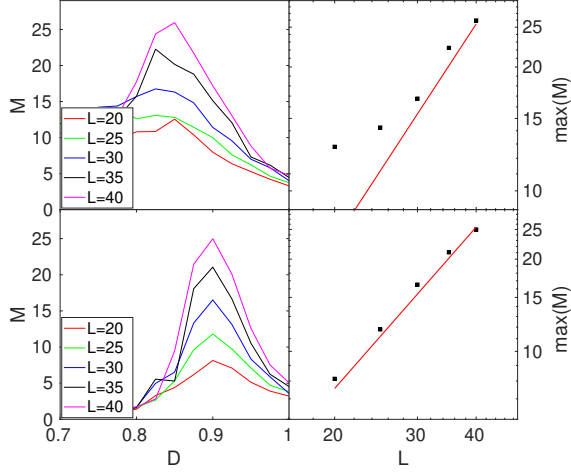conditions are periodic, as shown in the bottom panels of Fig. 11.

FIG. 11: Determination of the noise strength D_c corresponding to the critical temperature T_c for the GL equation in a 2-dimensional spatial domain. Left panels show the magnetization fluctuation M at steady state for different values of D and lateral system size L [magnet boundary conditions (top) and periodic boundary conditions (bottom)]. At $D = D_c$, corresponding to $T = T_c$, M diverges with L as $M \sim L^{\gamma/\nu} = L^{7/4}$ (red solid line) as expected from the 2D Ising critical exponents $\gamma = 7/4$ and $\nu = 1$ [36].

Appendix C: Dynamics without those realisations that interact with the upper boundary

In Fig. 12, the results of Fig. 3 are shown but discarding all realisations for which the surface profile touches the upper boundary at any given time. The ensuing plots agree with the interpretations and conclusions already derived from Fig. V.
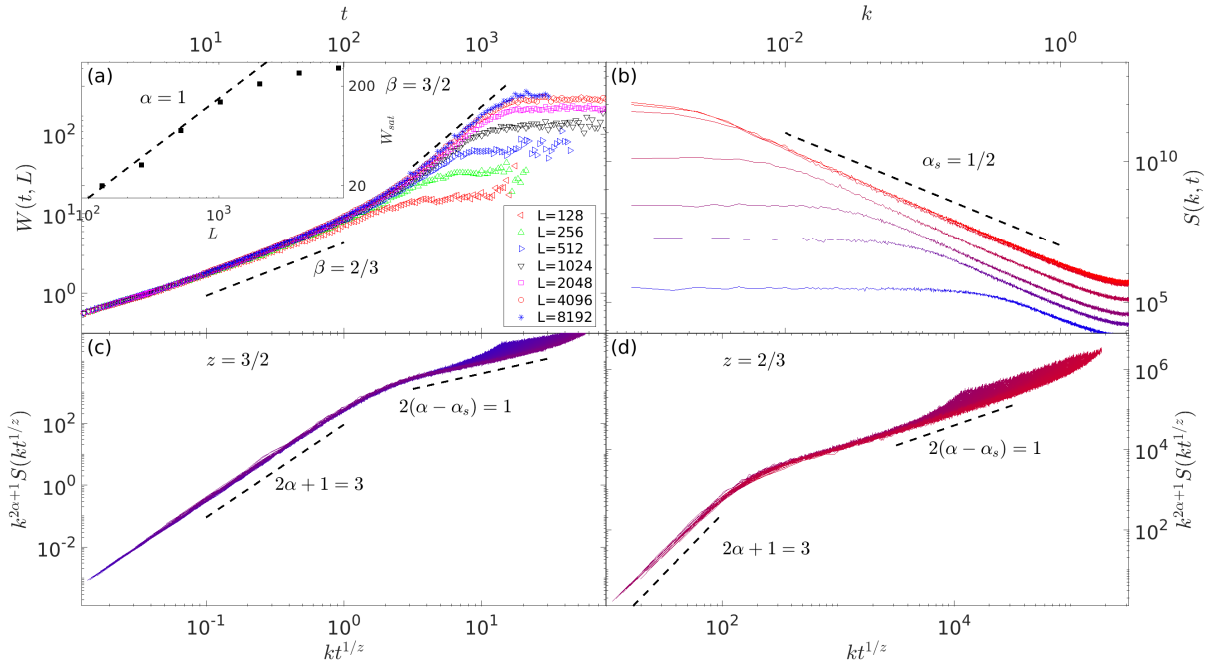
FIG. 12: Same as Fig. 3, but only using $h(x,t)$ data in which the fronts does not reach the upper system boundary at any point, time, or realization.

[1] S. Ramaswamy, *The mechanics and statistics of active matter*, Annu. Rev. Cond. Matter Phys. **1**, 323 (2010).

[2] M. C. Marchetti, J. F. Joanny, S. Ramaswamy, T. B. Liverpool, J. Prost, M. Rao, and R. A. Simha, *Hydrodynamics of soft active matter*, Rev. Mod. Phys. **85**, 1143 (2013).

[3] A. Polkovnikov, K. Sengupta, A. Silva, and M. Vengalattore, *Colloquium: Nonequilibrium dynamics of closed interacting quantum systems*, Rev. Mod. Phys. **83**, 863 (2011).

[4] H. Weimer, A. Kshetrimayum, and R. Orús, *Simulation methods for open quantum many-body systems*, Rev. Mod. Phys. **93**, 015008 (2021).

[5] U. C. Täuber, *Critical Dynamics* (Cambridge University Press, Cambridge, England, 2014).

[6] G. Grinstein, Generic scale invariance and self-organised criticality, in *Scale Invariance, Interfaces, and Non-Equilibrium Dynamics*, edited by A. McKane, M. Droz, J. Vannimenus, and D. Wolf (Springer, Cambridge, England, 1995).

[7] D. Belitz, T. R. Kirkpatrick, and T. Vojta, *How generic scale invariance influences phase transitions*, Rev. Mod. Phys. **77**, 579 (2005).

[8] A.-L. Barabási and H. E. Stanley, *Fractal concepts in surface growth* (Cambridge University Press, Cambridge, England, 1995).

[9] J. Krug, *Origins of scale invariance in growth processes*, Adv. Phys. **46**, 139 (1997).

[10] M. Kardar, G. Parisi, and Y.-C. Zhang, *Dynamic Scaling of Growing Interfaces*, Phys. Rev. Lett. **56**, 889 (1986).

[11] T. Kriecherbauer and J. Krug, *A pedestrian's view on interacting particle systems, KPZ universality and random matrices*, J. Phys. A: Math. Theor. **43**, 403001 (2010).

[12] I. Corwin, *The Kardar-Parisi-Zhang Equation and Universality Class*, Random Matrices: Theor. Appl. **1**, 1130001 (2012).

[13] T. Halpin-Healy and K. A. Takeuchi, *A KPZ Cocktail-Shaken, not Stirred...*, J. Stat. Phys. **160**, 794 (2015).

[14] K. A. Takeuchi, *An appetizer to modern developments on the Kardar-Parisi-Zhang universality class*, Physica A **504**, 77 (2018).

[15] Q. Fontaine, D. Squizzato, F. Baboux, I. Amelio, A. Lemaître, M. Morassi, I. Sagnes, L. Le Gratiet, A. Harouri, M. Wouters *et al.*, *Kardar-Parisi-Zhang universality in a one-dimensional polariton condensate*, Nature (London) **608**, 687 (2022).

[16] D. Wei, A. Rubio-Abadal, B. Ye, F. Machado, J. Kemp, K. Srakaew, S. Hollerith, J. Rui, S. Gopalakrishnan, N. Y. Yao, I. Bloch, and J. Zeiher, *Quantum gas microscopy of Kardar-Parisi-Zhang superdiffusion*, Science **376**, 716 (2022).

[17] F. Family and T. Vicsek, *Scaling of the active zone in the Eden process on percolation networks and the ballistic deposition model*, J. Phys. A: Math. General **18**, L75 (1985).

[18] P. Hohenberg and B. Halperin, *Theory of dynamic critical phenomena*, Rev. Mod. Phys. **49**, 436 (1977).

[19] M. Schroeder, M. Siegert, D. E. Wolff, J. D. Shore, and M. Plischke, *Scaling of growing surfaces with large local slopes*, EPL **24**, 563 (1993).

[20] S. Das Sarma, S. V. Ghaisas, and J. M. Kim, *Kinetic superroughening and anomalous dynamic scaling in nonequilibrium growth models*, Phys. Rev. E **49**, 122 (1994).

[21] J. M. López, M. A. Rodríguez, and R. Cuerno, *Superroughening versus intrinsic anomalous scaling of surfaces*, Phys. Rev. E **56**, 3993 (1997).

[22] J. J. Ramasco, J. M. López, and M. A. Rodríguez, *Generic Dynamic Scaling in Kinetic Roughening*, Phys. Rev. Lett. **84**, 10 (2000).

[23] M. Castro, R. Cuerno, A., Sánchez, and F. Domínguez-Adame, *Anomalous scaling in a nonlocal growth model in the Kardar-Parisi-Zhang universality class*. Phys. Rev. E **57**, R2491 (1998).

[24] J. M. López, M. Castro, and R. Gallego, *Scaling of Local Slopes, Conservation Laws, and Anomalous Roughening in Surface Growth*, Phys. Rev. Lett. **94**, 166103 (2005).

[25] H. Dashti-Naserabadi, A. A. Saberi, S. H. E. Rahbari, and H. Park, *Two-dimensional super-roughening in the three-dimensional Ising model*, Phys. Rev. E **100**, 060101(R) (2019).

[26] C. Cartes, E. Tirapegui, R. Pandit, and M. Brachet, *The Galerkin-truncated Burgers equation: Crossover from inviscid-thermalized to Kardar-Parisi-Zhang scaling*, Phil. Trans. R. Soc. A. **380** 20210090 (2022).

[27] E. Rodríguez-Fernández, Ph.D. thesis, Universidad Carlos III de Madrid (*unpublished*) (2022).

[28] E. Rodríguez-Fernández, S. N. Santalla, M Castro, and R. Cuerno, *Anomalous ballistic scaling in the tensionless or inviscid Kardar-Parisi-Zhang equation*, Phys. Rev. E **106**, 024802 (2022).

[29] C. Fontaine, F. Vercesi, M. Brachet, and L. Canet, *Unpredicted scaling of the one-dimensional Kardar-Parisi-Zhang equation*, Phys. Rev. Lett. **131**, 247101 (2023).

[30] J. Asikainen, S. Majaniemi, M. Dubé, and T. Ala-Nissila, *Interface dynamics and kinetic roughening in fractals*, Phys. Rev. E **65**, 052104 (2002).

[31] J. Asikainen, S. Majaniemi, M. Dubé, J. Heinonen, and T. Ala-Nissila, *Dynamical scaling and kinetic roughening of single valued fronts propagating in fractal media*, Eur. Phys. J. B **30**, 253 (2002).

[32] E. E. Mozo Luis, T. A. de Assis, and F. A. Oliveira, *Unveiling the connection between the global roughness exponent and interface fractal dimension in EW and KPZ lattice models*, J. Stat. Mech. 083202 (2022).

[33] M. E. Newman and G. T. Barkema, *Monte Carlo methods in statistical physics* (Clarendon Press, Oxford, 1999).

[34] J. Garcia-Ojalvo and J. M. Sancho, *Noise in Spatially Extended Systems* (Springer, Heildelberg, 1999).

[35] S. Taverniers, F. J. Alexander, and D. M. Tartakovsky, *Noise propagation in hybrid models of nonlinear systems: The Ginzburg-Landau equation*, J. Comput. Phys. **262**, 313 (2014).

[36] J. Cardy, *Scaling and Renormalization in Statistical Physics* (Cambridge University Press, Cambridge, 1996).

[37] See the Supplemental Material at XXX for a movie of the numerical simulation of Eq. (14), some snapshots of which are displayed in Fig. 2.

[38] B. G. Barreales, J. J. Meléndez, R. Cuerno, and J. J. Ruiz-Lorenzo, *Large-scale kinetic roughening behaviour of coffee-ring fronts*, Phys. Rev. E **106**, 044801 (2022).

[39] M. Nicoli, R. Cuerno, and M. Castro, *Unstable Nonlocal Interface Dynamics*, Phys. Rev. Lett. **102**, 256102 (2009).

[40] L. Gosteva, M. Tarpin, N. Wschebor, and L. Canet, *Inviscid fixed point of the multidimensional Burgers–Kardar-Parisi-Zhang equation*, Phys. Rev. E **110**, 054118 (2024).

[41] S. M. A. Tabei, A. Bahraminasab, A. A. Masoudi, S. S. Mousavi, and M. R. Tabar, *Intermittency of height fluctuations in stationary state of the Kardar-Parisi-Zhang equation with infinitesimal surface tension in d+1 dimensions*, Phys. Rev. E **70**, 031101 (2004).

[42] A. Bahraminasab, S. M. A. Tabei, A. A. Masoudi, S. S. Mousavi, and M. R. Tabar, *Zero tension Kardar-Parisi-Zhang*

equation in (d + 1)-dimensions, J. Stat. Phys. **116**, 1521 (2004).

[43] M. Castro, R. Cuerno, A. Sánchez, and F. Domínguez-Adame, *Anomalous scaling in a nonlocal growth model in the Kardar-Parisi-Zhang universality class*, Phys. Rev. E **57**, R2491 (1998).

[44] M. Castro, R. Cuerno, A. Sánchez, and F. Domínguez-Adame, *Multiparticle biased diffusion-limited aggregation with surface diffusion: A comprehensive model of electrodeposition*, Phys. Rev. E **62**, 161 (2000).

[45] M. Nicoli, M. Castro, and R. Cuerno, *Unified moving-boundary model with fluctuations for unstable diffusive growth*, Phys. Rev. E **78**, 021601 (2008).

[46] M. Castro, R. Cuerno, M. Nicoli, L. Vázquez, and J. G. Buijnsters, *Universality of cauliflower-like fronts: From nanoscale thin films to macroscopic plants*, New J. Phys. **14**, 103039 (2012).

[47] J. M. Marcos, P. Rodríguez-López, J. J. Meléndez, R. Cuerno, and J. J. Ruiz-Lorenzo, *Spreading fronts of wetting liquid droplets: Microscopic simulations and universal fluctuations*, Phys. Rev. E **105**, 054801 (2022).

[48] C. S. Dias, N. A. M. Araújo, and M. M. Telo da Gama, *Kinetic roughening of aggregates of patchy colloids with strong and weak bonds*, EPL, **107**, 56002 (2014).

[49] C. S. Dias, P. Yunker, A. Yodh, N. A. M. Araújo, and M. M. Telo da Gama, *Interaction anisotropy and the KPZ to KPZQ transition in particle deposition at the edges of drying drops*, Soft Matter **14**, 1903 (2018).

[50] P. J. Yunker, M. A. Lohr, T. Still, A. Borodin, D. J. Durian, and A. G. Yodh, *Effects of Particle Shape on Growth Dynamics at Edges of Evaporating Drops of Colloidal Suspensions*, Phys. Rev. Lett. **110**, 035501 (2013).

[51] M. Nicoli, R. Cuerno, and M. Castro, *Comment on "effects of particle shape on growth dynamics at edges of evaporating drops of colloidal suspensions"*, Phys. Rev. Lett. **111**, 209601 (2013).

[52] P. J. Yunker, M. A. Lohr, T. Still, A. Alexei, D. J. Durian, and A. G. Yodh, *Yunker et al. Reply*, Phys. Rev. Lett. **111**, 209602 (2013).

[53] T. J. Oliveira, and F. D. A. Aarão Reis, *Simulating the initial growth of a deposit from colloidal suspensions*, J. Stat. Mech. **2014**, P09006 (2014).

[54] F. Vercesi, S. Poirier, A. Minguzzi1, and L. Canet, *Scaling regimes of the one-dimensional phase turbulence in the deterministic complex Ginzburg-Landau equation*, Phys. Rev. E **109**, 064149 (2024).

[55] P. H. R. dos Anjos, M. S. Gomes-Filho, W. S. Alves, D. L. Azevedo, and F. A. Oliveira, *The Fractal Geometry of Growth: Fluctuation–Dissipation Theorem and Hidden Symmetry*, Front. Phys. **9**, 741590 (2021).